Amol University of Special Modern Technologies

Caspian Journal of Engineering Modern Technologies

Journal homepage: https://cjemt.ausmt.ac.ir/

Research Article

Analysis and Design of Photonic Band Gap Devices: A Review

Roberto Marani[1] and Anna Gina Perri[2,*]

[1]Institute of Intelligent Industrial Technologies and Systems for Advanced Manufacturing (STIIMA), National Research Council of Italy, 70125, Bari, Italy
[2]Electronic Devices Laboratory, Department of Electrical and Information Engineering, Polytechnic University of Bari, 70126, Bari, Italy

(*) Corresponding author: annagina.perri@poliba.it

Paper INFO

Paper history:
Received: 2023-07-11
Accepted: 2023-10-15

Keywords:
Photonic Band Gap Devices;
Modelling;
Resonant Cavity Design;
Particle Accelerator Design.

ABSTRACT

Photonic BandGap (PBG) crystals are able to overcome the typical integration limits of traditional optical circuits, allowing a scale of integration similar to the electronic ULSI. According to their geometrical characteristics, photonic crystals inhibit the light propagation in one or more directions, depending on the working frequency: if so, a band gap exists, i.e. a frequency range in which the wave cannot propagate. Moreover, the introduction of defects inside the periodical structure of a photonic crystal determines the forming of photonic states located in the gap. In this paper, after a brief description of operation principle of photonic crystals, we present a review of the most important photonic crystals devices, describing, in particular, the main steps required to model and design resonant cavities and particle accelerators.

1. INRODUCTION

The Internet spreading has carried to an increasing request of wider band and electronic integration for telecommunication network. This aspect led to define technologies, as Photonic Band Gap (PBG) crystals, in order to obtain a faster data treatment. PBG crystals are able to overcome the typical integration limits of traditional optical circuits, allowing a scale of integration similar to the electronic ULSI.

PBG crystals are materials able to influence the light propagation analogously it occurs for the propagation of the electrons in semiconductors.

In fact, in a semiconductor the crystal lattice causes the formation of a periodic potential for an electron which propagates through it. This periodicity determines the formation of energy band gaps for the electronic states, that is of energy bands forbidden to the propagating electrons.

In photonic crystals, to propagate some light quanta (or photons) a principle similar to what is seen for the semiconductor crystals will be exploited, as the crystal periodicity is artificially realized by means of alternation of dielectric macroscopic materials.

According to their geometrical characteristics, photonic crystals inhibit the light propagation in one or more directions, depending on the working frequency: if so, a band gap exists, i.e. a frequency range in which the wave cannot propagate. The bandgap is complete if – to those frequencies – the propagation is prevented in all the possible directions.

The introduction of defects inside the periodical structure of a photonic crystal determines the forming of photonic states located in the gap. Such characteristic is exploited to carry out devices with high capabilities, for example optical micro-resonators (in which a column is removed) or low losses waveguides, which are based on the presence of a bandgap and not on the total internal reflection.

In this paper, after a brief description of operation principle of photonic crystals, we present a review of the most important photonic crystals devices, describing, in particular, the main steps required to model and design resonant cavities and particle accelerators.

2. PBG-BASED STRUCTURES

Figure 1 shows different PBG-based structures, characterized by mono-dimensional (1-D), bidimensional (2-D) or tridimensional (3-D) periodicity, each of them infinitely extended and then so-called *bulk*. On the contrary, Figure 2 shows wave-guiding periodic structures, characterized by a finished thickness and a 1-D, 2-D or 3-D periodicity.

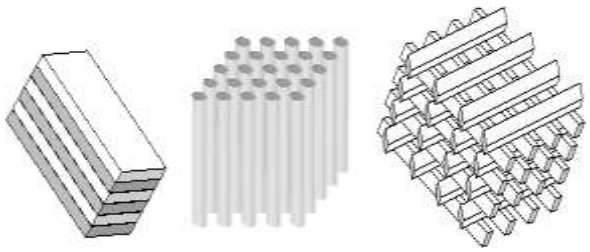

Figure 1*. Bulk 1-D, 2-D and 3-D photonic crystals.*

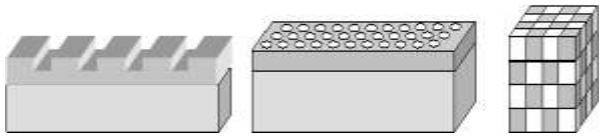

Figure 2*. Wave-guiding 1-D , 2-D and 3-D structures.*

A wave incident on a dielectric discontinuity is partially reflected, partially transmitted and partially diffracted. We

can then distinguish between two waves, one propagating in a positive direction and the other in a negative direction. If the wave is incident on a periodic structure, the produced waves can – in particular conditions – destructively interfere and propagation is then inhibited, then a bandgap appears.

The characterization of a photonic crystal is carried out through the so-called *Brillouin diagrams*, where the frequency of the allowed electromagnetic modes is plotted as a function of the normalized propagation constant in all directions of the irreducible Brillouin zone.

Figure 3 shows a frequency range (i.e. bandgap), between the dashed lines, in which no propagation can occur.

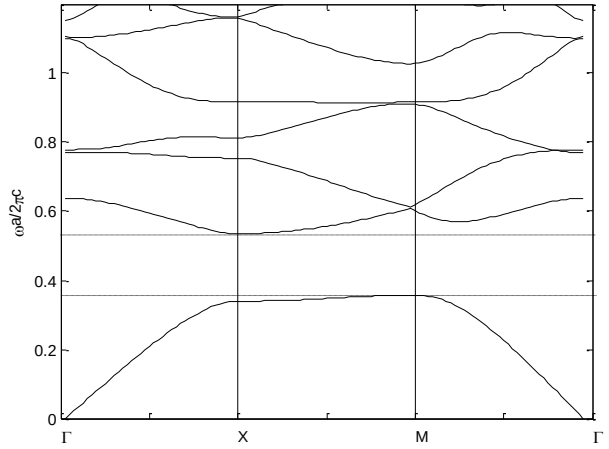

Figure 3*. Photonic band of a PBG structure having lattice vector a and with different thickness layers. The thickness of the layers at high index is 0.2 a and that of the layers at low index is 0.8 a (a is the grating constant).*

The frequency range in which the wave is particularly concentrated in the high refractive index medium is called *dielectric band*, while the other one is called *air band*.

In Figure 4 a lattice of circular rods is shown; the material is homogeneous in z direction and periodic in the plane x-y, being *a* the grating constant. The grating is arranged according a square cell array, as shown in the inset of the same Figure 4.

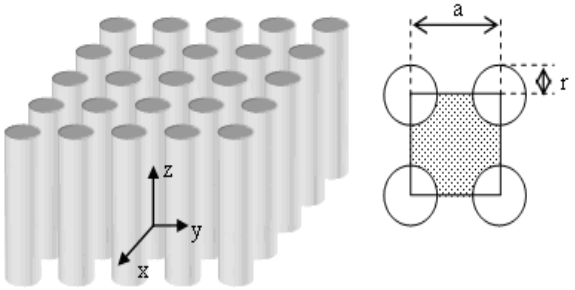

Figure 4*. 2-D PBG.*

The physical characteristics of the described structure are determined by its design parameters: the grating constant, the *filling ratio*, the rod radius, the geometry of

the unit cell, the refractive index contrast.

The filling factor gives a measure of the electromagnetic energy located inside the high index dielectric regions in comparison with the energy distributed in the whole volume, being large in the dielectric band and small in the air band.

The photonic investigation of the described structure, having rod radius equal to 0.2 a, shows a different behaviour for TE and TM modes, as depicted in Figure 5.

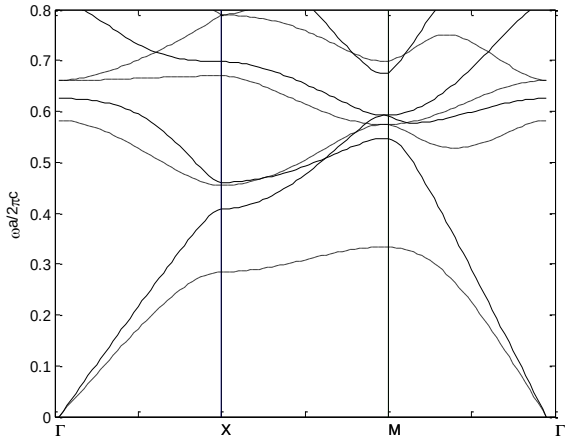

***Figure 5**. Brillouin diagram for a squared array of dielectric columns having r = 0.2 a for TE modes (solid line) and TM modes (dashed line).*

In particular, there is a complete bandgap for TM modes, while TE modes can always propagate for each frequency.

The structure constituted by a square array of high dielectric columns has a complete bandgap for the TM modes but not for the TE ones for the following reasons:

- the mode mainly localized in the high refractive index medium has a frequency lower than the one of the mode concentrated in the low refractive index medium: this explains the bandgap formation (separation in ω);
- TM modes have the Maxwell displacement vector D orthogonal to the periodicity plane and, then, localized in the high refractive index regions;
- for the TE modes the Maxwell displacement vector D is oriented in the periodicity plane and must necessarily enter into the low index regions (for both the air and dielectric bands), thus resulting in a smaller separation among the bands in comparison with the TM ones.

The wave behaviour changes if the type of used structures varies.

For example, a structure with square section rods at low index has characteristics, in terms of bandgap, opposite to those of a structure with circular section rods. In fact:

- the squared structure offers a continuous path among the high index regions: the field, orthogonal to the periodicity plane in the TM modes, is concentrated in the crossings among the high index bars (dielectric band) or inside the high index bars (air band). It follows that the field configuration is similar for both the bands and, so, the separation between them is small;

- for the TE modes the D field is contained in the periodicity plane and localizes inside the high index regions in the dielectric band while, presenting nodes in the high index bars, it must necessarily penetrate into the low index regions to place itself in the air band structure, with a consequent greater bandgap in comparison to the TM case.

According to the investigated structures the general design rules, useful to establish the necessary conditions for a complete bandgap, can be determined:

- not connected regions of high refractive index materials improve the bandgap for TM modes;
- connected regions of high refractive index material improve the bandgap for TE modes;
- a hexagonal cell of air columns carries out both the previous characteristics, thus providing a complete bandgap for both the polarizations;
- for strong index contrasts even a square cell of air columns presents a complete bandgap.

The following photonic band diagram, shown in Figure 6, calculated for a structure having a triangular cell of air columns drilled in a semiconductor substrate, shows a complete bandgap for both TE and TM modes.

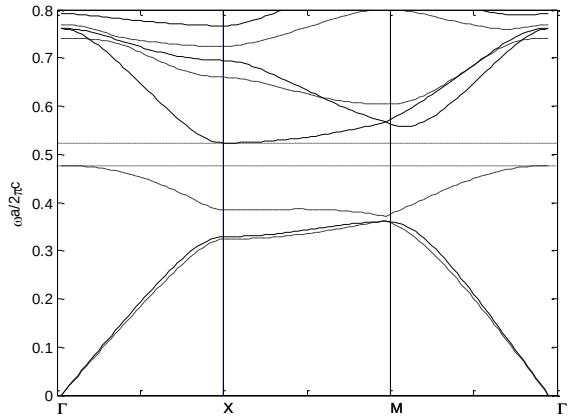

Figure 6*. Photonic diagram for a structure having a triangular cell of air columns drilled in a semiconducor substate. A band gap for both polarizations is shown.*

In particular, there is a complete bandgap for TM modes, while TE modes can always propagate for each frequency.

A 3-D crystal has an almost infinite numbers of geometries, but only few of them having a complete bandgap. A typical 3-D structure is the opal (Figure7), constituted by high index spheres in a low index background or vice versa (inverted opal).

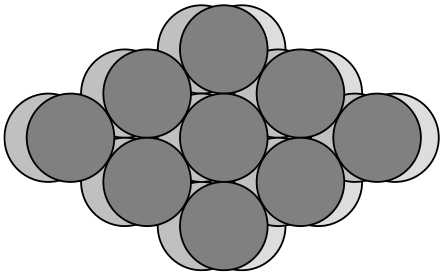

Figure 7*. 3-D PBG opal.*

The spheres can be arranged in a suitable manner, thus reproducing a general crystal structure.

In all the cases the basic condition to obtain a complete bandgap is that the regions at high and low index are connected.

3. MATHEMATICAL MODELS OF PHOTONIC CRYSTALS

The fundamental equation obtained from Maxwell equations, which must be solved for the solution of the electromagnetic problem is:

$$\left\{\nabla \mathrm{x} \frac{1}{\varepsilon(\mathbf{r})} \nabla \mathrm{x}\right\} \mathbf{H(r)} = \omega^2 \mathbf{H(r)} \qquad (1)$$

which is an eigenvalues equation, similar to the Schröedinger equation. Hence the idea that, if the permittivity function represents a crystal constituted by macroscopic *atoms* placed periodically, the photons propagating in the crystal must be describable in terms of structure with photonic bands and of Bloch functions, analogously to what happens in the semiconductors for the electrons.

Eq. (1) of the photonic crystals can be solved in both time and frequency domain.

3.1. Methods in the Frequency Domain

The magnetic field **H** is expanded in a series of harmonics and the equation can be rewritten in the following form:

$$\Theta \mathbf{H}_n = \lambda_n \mathbf{H_n}$$

$$\Theta \mathbf{H_n(r)} = \left\{\nabla \mathrm{x} \frac{1}{\varepsilon(\mathbf{r})} \nabla \mathrm{x}\right\} \mathbf{H_n(r)}$$

where Θ is the hermitian operator. The problem is therefore to find all the eigenvalues λ_n.

3.2. Methods in the Time Domain

The Maxwell's equations are written in the time domain:

$$\nabla \mathbf{xE(r,t)} = -\frac{\partial \mathbf{H(r,t)}}{\partial \mathrm{t}}$$

$$\nabla \mathbf{xH(r,t)} = \boldsymbol{\varepsilon}(\mathbf{r}) \frac{\partial \mathbf{E(r,t)}}{\partial \mathrm{t}}$$

and can be solved by using a numerical method providing the following steps:

1. the equations are discretized within an elementary cell;
2. the time domain is discretized by arbitrarily choosing the discretization step;
3. the derivatives are approximated in every point of the cell with a finite difference (finite difference methods);
4. the field can then be investigated as a function of the time, thus allowing the analysis of microcavities and, in particular, of essential parameters such as scattering, coupling efficiency and quality factor.

The solution of Maxwell equations based on algorithms in the time domain allows to calculate the band structure too. The field in the nodes out of the domain in the selected calculation is connected with the field in the nodes in the domain through the Bloch condition [1]:

$$\mathbf{E(r+a},t) = e^{\mathbf{jka}}\, \mathbf{E}(\mathbf{r},t)$$

where **r** is the position vector of a fixed node in the discretized domain (elementary cell), **a** is the grating constant, **k** is the wave vector.

The most important numerical methods used to solve the equation of photonic crystals are the following:

1. Transfer Matrix Method (TMM) [2]
2. Plane Wave expansion Method [3]
3. Bloch Wave Method (BWM) [4]
4. Finite Difference Time Domain Method (FDTD) [5]
5. Bi-directional mode expansion and propagation method (BEP) [6]

6. Scattering Matrix Method (SMM) [7]
7. Leaky Mode Propagation method (LMP) [8].

4. DEFECTS AND DEVICES ON PBG

The introduction of defects inside the periodical structure of a photonic crystal determines the forming of photonic states located in the gap. Such characteristic is exploited to carry out devices with high capabilities, for example optical micro resonators (in which a column is removed) or low losses waveguides, which are based on the presence of a bandgap and not on the total internal reflection.

The behaviour of a defective photonic crystal is analogous to that of a doped semiconductor, which is characterized by the presence of allowed states for the electrons inside the forbidden band near the conduction or the valence bands, depending on the kind of impurities embedded in the semiconductor.

In a monodimensional structure the defect is constituted by a missing layer, or a layer having a width different from the others, as shown in Figure 8.

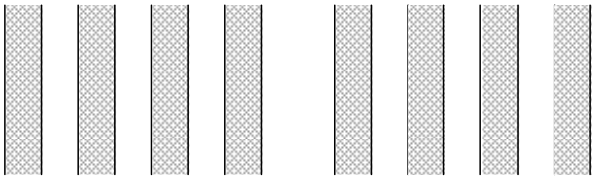

Figure 8*. Defect in a 1-D photonic crystal.*

If the defect has a suitable width, an allowed state is provided inside the bandgap, thus resulting in a strong localization of the mode, which exponentially vanishes into the sourrounding periodical regions.

The presence the 1-D defect provides a phase shift of an odd multiple of π [9] for a complete oscillation (backwards and forwards)**.** It follows that the allowed states exist only at discrete energies and the corresponding resonance frequencies decrease with increasing the defect size.

The transmission curve is also modified at the allowed state wavelength showing a maximum, as shown in Figure 9.

Fabry-Perot passband filters can be also designed by using defective 1-D PBG based structures.

In 2-D photonic crystals a single defect is achieved by removing a rod from the lattice (Figure 10) or replacing it with another one of different refractive index material (Figure 11).

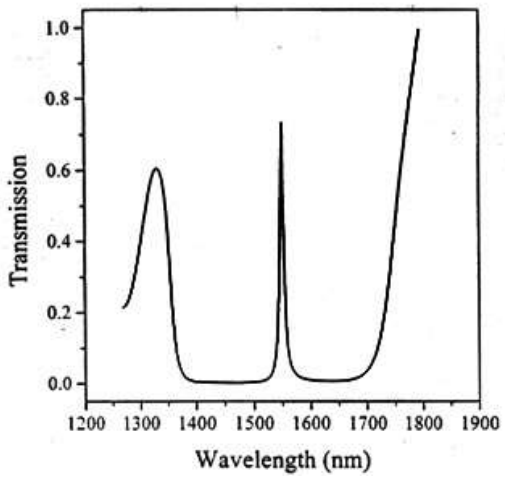

Figure 9*. Transmission coefficient in presence of a defect to λ/4.*

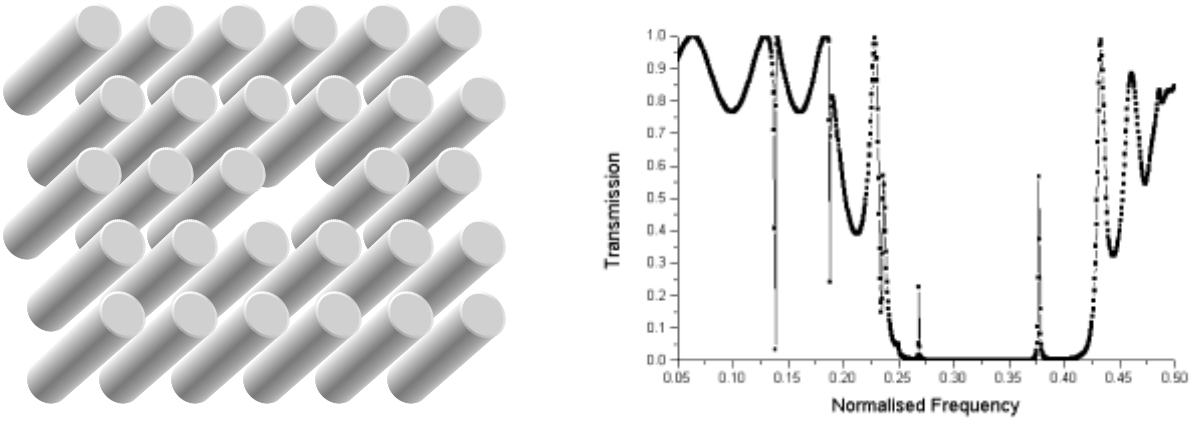

***Figure 10**. 2-D photonic crystal with defect obtained by removing a dielectric rod and its transmission spectrum.*

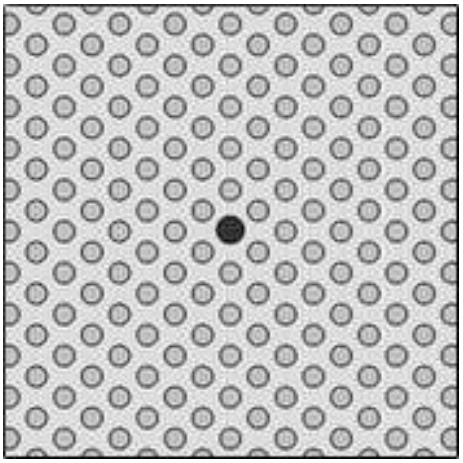

***Figure 11**. Defect obtained by using an high refractive index rod.*

The presence of a defect determines a transmission peak inside the forbidden band and produces a concentration of field in the defective region, thus creating a bidimensional cavity surrounded by reflecting walls supporting an allowed state inside the bandgap.

Instead, in a 2-D PBG, line defects can be realized by removing one or more sets of rods.

A waveguide is realized by making a defective path, where the light can be confined since no propagation in the surrounding crystal can occur, thus decreasing propagation losses. This feature can be advantageously used to realize strongly curved waveguides.

Figure 12 shows the architecture of several PBG-based optical devices.

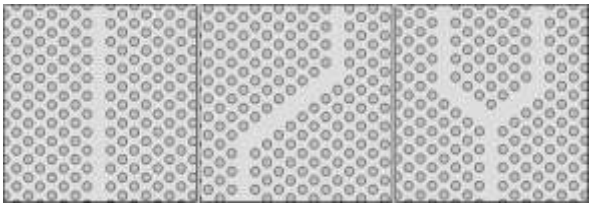

***Figure 12**. Different structures realized with line defects. a) straight, b) curved waveguide c) Y-branch.*

It is possible to introduce some irregularities in the grating of a 3-D crystal:

1. by adding a material with different dielectric constant in the unitary cell (dielectric defect);
2. by removing part of the dielectric material from the unitary cell air defect.

In the first case the defect behaves analogously to a donor atom in an ordinary crystal, thus producing an allowed state (*donor mode*) near the lower edge of the air band.

Similarly, an air defect is similar to an acceptor atom, and localizes the field distribution (*acceptor mode*) near the upper edge of the dielectric band. These defects are particularly interesting for realizing resonant microcavities with high Q.

Some theoretical investigations [10] show that the frequency of the acceptor mode increases with increasing the removed material volume, while a small amount of volume results in an acceptor level near the edge of the dielectric band. Moreover, a too small amount of removed material push localized states within a continuum of levels below the top of dielectric band.

Similarly, a donor level requires a minimum removed volume for creating an allowed level below the air band edge. In this case, the frequency of the donor level diminishes with increasing the defect volume.

In a 3-D crystal it is possible to localize the light in a single region by introducing a point defect. This behaves as an entirely reflecting walls resonant cavity, which the electromagnetic field is confined into. Outwardly the defect the field will vanish along the three dimensions of the crystal.
Besides point defects, linear type defects can also be realized by creating a whole defective region which extends in the crystal [11] . This approach allows to fabricate high quality waveguides, able to confine the light and to make negligible losses also at optic frequencies.

5. APPLICATIONS OF PBG-BASED DEVICES

The first PBG was fabricated by Yablonovitch [10-11], characterized by a bandgap only at microwave frequencies because of technological limitations (to work with smaller wavelengths, a smaller rod size is required). The 2-D bulk crystal was obtained by drilling the silicon according a face centred cubic (FCC) arrangement being this architecture the simplest and most suitable for achieving a complete bandgap (in all directions and for all polarizations), as suggested by theoretical studies.

Actually, the most important applications are:

- waveguides, power splitters and switches with low losses over long distances and in presence of strong bends;
- optical fibres, monomodal in a wide range of wavelength, with a low core refractive index. Only the mode that satisfies the Bragg condition can propagate;
- perfectly reflective mirrors, in particular for laser cavity walls;
- LED diodes having very high external efficiency (4% without PBG) because only the emission of the transmittable modes occurs. All the emitted energy is then transmitted;
- laser diodes having low threshold (<100 μA): since the spontaneous

emission is suppressed, because photons having energy inside the band-gap are not emitted, the related loss decreases, the efficiency increases, the dissipated power decreases;

- narrow band filters for DWDM (Dense Wavelength Division Multiplexing) systems;
- resonant cavities with very high *Q*-factor;
- biomedical sensing applications based on porous silicon;
- particle physics applications to realize high spectral purity accelerators;
- photonic integrated circuits: PBG allow to reduce photonic circuits sizes (up to a few hundred of squared μm) because:
  - laser beam can propagate through strongly bent guides with very low losses;
  - LED and laser high efficiency allows a low power consumption and, then, the integration in very small areas;
  - the power coupling among adjacent waveguides is strongly reduced;
  - superprism effects can be used.

In particular, in the following Sections, we examine the PBG applications related to the design of resonant cavities and particle accelerators.

6. DESIGN RULES OF RESONANT CAVITIES

Conventional microwave resonant cavities are boxes enclosed by conductive walls containing oscillating electro-magnetic fields. Conductive walls act as perfect screens, therefore avoiding any radiation of energy away from the box. Because of the large extension of inner walls, current density and losses are reduced.

Optical resonators are rather different from the microwave typical ones for the smaller operative wavelength, which yields a large number of allowed modes. Although there are several and important differences between optical and microwave resonators, some parameters, as quality factor *Q*, are very useful for both kind of cavities. The quality factor *Q* is defined as:

$$Q = \omega_0 U/W$$

where ω_0 is the resonance frequency, *U* the electromagnetic energy stored in the cavity and *W* the lost power. Losses in the dielectric material and radiations from small apertures can cause the lowering of *Q*.

The *Q* factor allows to evaluate also the filter bandwidth, defined as:

$$\Delta\omega/\omega_0 \cong 1/Q$$

where $\Delta\omega$ is the range between two frequencies at which the signal power is 3 *dB* lower than the maximum value. It can be shown that, at a given frequency, the *Q*-factor increases with an increasing order of mode.

A resonant cavity can be obtained by introducing a defect in a photonic crystal in order to modify its physical properties. In the case of a defectless structure, electromagnetic waves cannot propagate when the operative frequency is inside the bandgap, in which a narrow band of allowed frequencies can be achieved breaking the crystal periodicity through a suitable defect.

Light localization is used in the PBG based microcavity design to optimize the *Q*-factor, which depends on the geometrical and physical properties of the defect. Lattice defects are constituted by

dielectric regions of different shapes, sizes or refractive index values. By changing one of these parameters in the defective region we can modify the mode number of the resonance frequency inside the cavity. Moreover, the spectral width of the defect mode is demonstrated to decrease rapidly with an increasing number of repetitions of the periodic structure around the cavity region, so improving the selectivity of the resonance frequency inside the bandgap.

The excellent performances of PBG structures have been used to develop resonators characterized by high values of *Q*-factor working at microwave frequencies, by introducing defects in 3D and particularly in 2D structures. Microwave resonant cavities are constituted by dielectric materials and metals, thus keeping the same fundamental properties of the PBG structures. Metallic structures are easier and less expensive to realize and can be used for accelerator-based applications. Most interesting 2D and 3D devices have a geometrical structure that allows a large bandgap, achieved by using a triangular cell for 2D or woodpile cell for 3D structures, with an efficient wake-field suppression at higher frequencies, without interfering with the working mode.

In microwave applications the use of carbon-based low losses materials (Duroid, Teflon), aluminium oxide or highly resistive silicon is already described in literature. In particular highly resistive silicon has been demonstrated to be most suitable at frequencies near 100 GHz [12-15]. Moreover, both dielectric and metallic-dielectric gratings have been investigated, thus achieving an improvement in terms of *Q*-factor.

The final architecture is constituted by a 2D triangular lattice, in which a rod at the centre has been removed (defect), thus producing a resonant cavity (Figure 13). To localize the mode, three rows of rods have been used, and all the rods are confined inside a metallic cylinder closed on both ends.

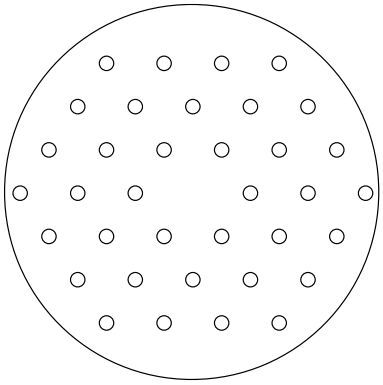

***Figure 13**. Architecture of the PBG cavity.*

The main difference with traditional cavities is the absence of coupling holes, at the opening of waveguide, which produce a down-shift frequency of 2%. PBG-based cavities are not affected by this problem because of the distributed cavity coupling.

In fact, fields are confined by the rods nearest to the defect, and these rods are not perturbed in order to obtain the coupling.

The main steps required to design a resonant cavity are:

- design of the periodic structure to obtain a suitable bandgap around the required working frequency;
- creation of a defect in the grating to establish a defect mode;
- analysis of higher order modes that have to be not confined, being in the crystal passband, and thus can be absorbed by coatings at the edge of the structure;
- design of a suitable hole in the central region of the plates to allow the propagation of the accelerated beam outside the device.

7. DESIGN RULES OF PARTICLE ACCELERATORS

Traditional particle accelerators can be considered as metallic waveguides that carry TM_{01} mode, thus producing the highest acceleration for a given working power, but even suffering from the excitation of higher order modes (HOM) at high frequencies. Moreover, metallic walls produce absorption losses that increase with the frequency [16].

PBG-based resonant cavities are used in particle accelerator applications, with drastic improvement of performances. The structure is formed by three triangular cell gratings, separated by superconductor layers. Each grating has a defect, obtained by removing a rod. The hole at the centre of conductor layers allows the particle beam emission.

In fact:

- PBG can substitute the metallic walls, obtaining perfectly reflective surfaces without absorption losses;
- PBG allows the suppression of higher order modes in the resonant cavity of the accelerator;
- since the field in a PBG based cavity is strongly confined in a very small region, wider tolerances become acceptable on the material quality, which has to be very high in the centre of the cavity – where the field is confined – but can be lower in the outer regions. This aspect is very important when a superconductor material is used, since semiconductors have not a uniform high quality on large surfaces;
- straight structures can be realized and high accelerations obtained;
- it is possible to optimize the coupling between the resonant cavity and the input waveguide, thus reducing the resonance frequency shift which is a typical problem of a standard pillbox cavities.

The presence of a defective region, in which the periodicity is not regular because one or more rods are missing, produces a strong electromagnetic field localization at a given frequency, which depends on the characteristics of the defect. The bandwidth of the defect is related to the *Q*-factor, so it is possible to make resonators with high *Q*-value and high suppression of the higher order modes.

The main design parameters are: height, diameter and rods number, distance between rods centres, geometry and thickness of plates. In any case, the design statements are related to the application of these accelerant cavities.

8. DESIGN OF PBG-BASED ACCELERATING CAVITY

In order to take into account all effects due to the shape of the accelerating cavity, we consider two different architectures both constituted by either dielectric or metallic rods arranged according a 2D periodic triangular lattice, embedded in air and sandwiched between two ideal metal layers. In this way only TM modes are excited.

The investigated structures are shown in Figure 14.

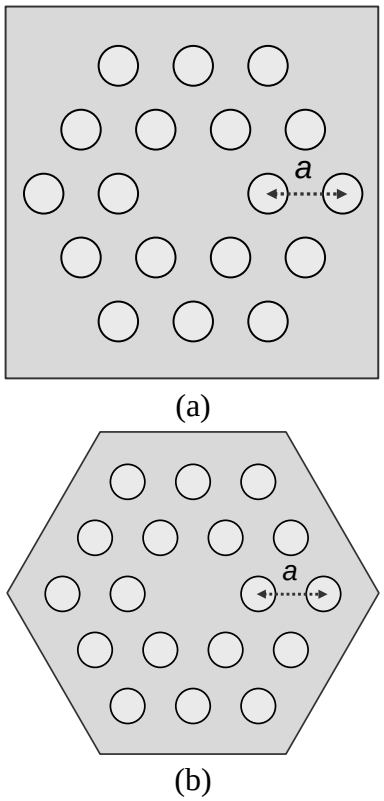

***Figure 14**. Accelerator with squared external wall (a) and hexagonal external wall (b).*

The aim of the analysis is to find the optimal geometrical parameters for placing the operating resonance frequency close to the centre of the bandgap. Once the lattice parameters have been determined, the central rod must be removed to create the resonance condition, thus providing a localized state inside the bandgap.

The analysis makes use of a rigorous formulation of the Quality Factor according to the Floquet-Bloch formalism, to investigate the photonic behaviour of the resonant cavity.

We assume rod radius *R*, lattice constant *a* (see Figure 14) and rod height t_g.

To evaluate the Q-factor, previously defined, it is necessary to calculate the energy *U* stored by the electromagnetic field and the lost power *W*.

The electromagnetic field energy is given by:

$$U = \frac{\mu_0}{2}\int_V H^2 dv$$

where *H* is the magnetic field amplitude, μ_0 is the vacuum permittivity and the integral are extended over the cavity volume.

Since the periodic structure is sandwiched between two ideal metal layers, only TM modes can be excited, being the electric field perpendicular to the periodicity plane and all the field components constant with respect to the cavity height. In this case the electromagnetic field energy can be rearranged as:

$$U = l\frac{\mu_0}{2}\int_S H^2 ds$$

where *l* is the height of the cavity and *S* is the cavity cross section.

The lost power *W* can be written as follows:

$$W = l\frac{1}{2}R_s\int_l H^2 dl + 2\frac{1}{2}R_s\int_S H^2 ds.$$

Where R_s is the metal surface resistance. In the previous relationship the first term

takes into account the lost power due to the currents on the rods, while the second term evaluates the losses due to currents on the metal layers. By putting:

$$\delta = \frac{2R_s}{\omega\mu_0} \text{ and } R_{eff} = 2\frac{\int_S H^2 ds}{\int_l H^2 dl}$$

we obtain:

$$Q = \frac{1}{\delta\left(\frac{1}{R_{eff}} + \frac{1}{l}\right)}$$

This relationship can be used also for superior order modes supported by the structure, if all fields are constant along the rod height.

The Q factor can be written as:

$$\frac{1}{Q} = \frac{1}{Q_\delta} + \frac{1}{Q_{met}}$$

where Q_δ is the quality factor taking into account losses in the dielectric medium, while Q_{met} accounts for the ohmic losses due to the currents on metallic walls. Moreover:

$$Q_\delta = \frac{1}{k(\tan\delta)}$$

where k is the fraction of the energy stored in dielectric rods, while $\tan\delta$ is the loss tangent due to the dielectric medium. For our calculations we have assumed $\tan\delta$ is equal to 10^{-4}.

9. NUMERICAL RESULTS

As first step we have investigated the physical properties of a microwave 2D periodic structure in terms of forbidden frequencies.

The designed parameters values are:

a = 8.58 *mm*, R = 1.5 *mm*, t_g = 4.6 *mm*, ε_a = 9, ε_b = 1.

The photonic band diagram shows the first bandgap extending from 12.7 *GHz* to 20.15 *GHz*.

In order to take into account the defect presence, constituted by a rod missing (see Figure 14), several simulations have been performed by using a FEM (Finite Element Method) based approach, thus computing both field distributions and *Q*-factors for different configurations.

Figure 15 shows the first three modes for the electric field E_z component.

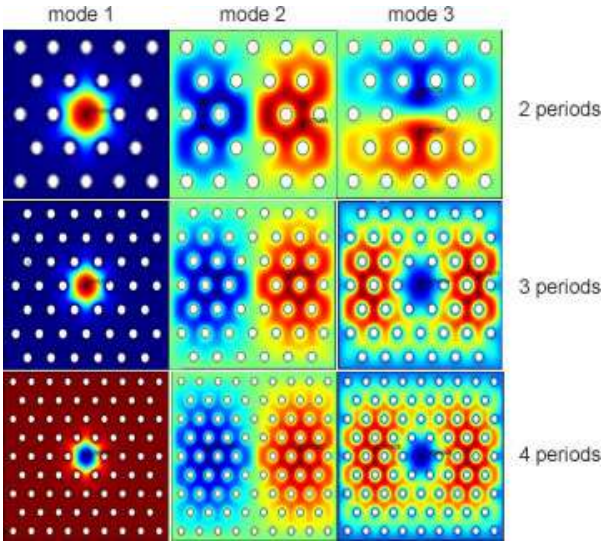

***Figure 15**. Electric field component E_z for 2, 3 and 4 grating periods.*

Modes have been computed for two, three and four grating periods, not showing any difference in the first mode which is well confined in the defect space also for two grating periods. Of course the increase of grating periods does not change the distribution of the first mode, but becomes very significant for high order modes which are distributed externally with respect to the defect space and suffer from losses due to the third grating period.

This aspect can be noticed from Table 1, in which two different accelerators are compared, the first one with external squared wall (Figure 14a), the second one with external hexagonal wall (Figure14b). Both accelerators have the same periodic structure with metallic rods. In the first

column of the Table 1 the number of grating periods is reported. The change of both the first mode resonant frequency and quality factor with increasing the period number is negligible. On the contrary, high order modes are external to the defect and suffer from any further grating period thus producing an additional loss and a consequent decrease in the *Q*-factor.

Table 1. *Comparison between two accelerators.*

		Squared wall		Hexagonal wall	
N	mode	Frequency (*GHz*)	Q	Frequency (*GHz*)	Q
2	1	14.1594	4434.3	14.1598	4439.0
	2	20.5393	3721.5	21.0130	4091.0
	3	20.8323	3893.7	21.0130	4091.7
3	1	14.1592	4436.2	14.1592	4432.1
	2	20.2662	3445.6	20.5412	3592.5
	3	20.3322	3427.0	20.5412	3592.4
4	1	14.1592	4430.9	14.1592	4431.7
	2	20.1152	3335.0	20.2944	3342.8
	3	20.1177	3314.5	20.2959	3403.3

In the Table 2, a comparison between particle accelerators, based on a triangular cell array and an external hexagonal wall, is shown.

The two structures have been designed with dielectric and metallic rods, respectively. Of course, only two grating periods are required for localizing the first mode, thus reducing every further loss. The structure characterized by dielectric rods does not suffer from any reduction of performances due to the increase of the number of grating periods, both for the first mode and high order modes. In fact, the dielectric rods improve the quality factor with respect to the same structure with metallic rods, which are characterized by strong resistive losses.

Figure 16 shows the Ez field component distribution in the hexagonal cavity.

In Figure 16 the first mode is shown in case of metallic rods (first row) for two, three and four grating periods. The same mode is sketched for dielectric rods (second row), thus showing a different field distribution.

***Table 2**. Comparison between two accelerators, based on a triangular cell array and an external hexagonal wall.*

		Dielectric rods		Metallic rods	
N	mode	Frequency (*GHz*)	Q	Frequency (*GHz*)	Q
2	1	14.9091	7018.3	14.1598	4439.0
	2	18.8251	6877.4	21.0130	4091.0
	3	19.1886	7128.9	21.0130	4091.7
3	1	14.8314	7142.2	14.1592	4432.1
	2	18.4442	7020.8	20.5412	3592.5
	3	18.5926	7068.8	20.5412	3592.4
4	1	14.8216	7163.0	14.1592	4431.7
	2	18.2596	7056.2	20.2944	3342.8
	3	18.3614	7096.1	20.2959	3403.3

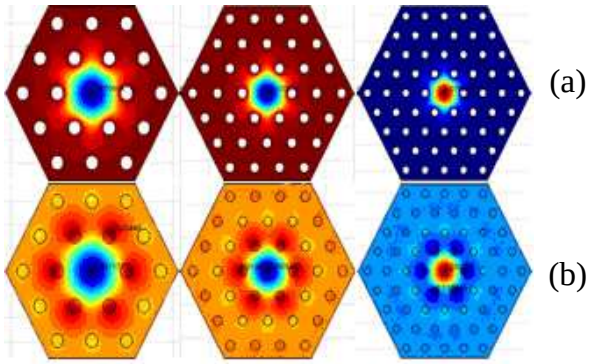

***Figure 16**. First mode for metallic rods (a) and dielectric rods (b).*

10. PROTOTYPE REALIZATION AND MEASUREMENTS

We have realized the copper prototype, shown in Figure 17, at the Electronic Devices Laboratory of Polytechnic University of Bari (Italy).

The difference between the theoretical results and those obtained by measures are related to the actual realization tolerances that, in this case, are limited to 0.1 mm, and the inaccuracy of the experimental characterization. This implies that cylinders are placed in different position, not vertically aligned, with rough surfaces, etc.

Secondly, the cavity is made of 36 cylinders enclosed between two copper plates. Thus the contact resistance between elements is added to the copper resistivity with an increasing value of losses with respect to the preliminary theoretical investigation and a consequent decrease of the *Q*-factor.

Figure 17*. Prototype images. Dimensions are compared with a pen and a PC-mouse.*

Finally, a 5 *mm* diameter hole has to be placed on each plate near the central defect region, in order to get the correct measures. As shown in Figure 18, the network analyzer HP 8720ES has been implemented to measure the *s*-parameters for the experimental characterization of the prototype.

Figure 18*. Network Analyzer HP 8720ES with excitation and measure probes.*

By setting the spectrum analyzer [17] in a frequency range between 12 and 20 *GHz* and a bandwidth at intermediate frequency (IF bandwidth) of 10 *Hz* (minimum value that allows to remove noise), the s_{11} and s_{21} parameters are measured, as shown in Figure 19.

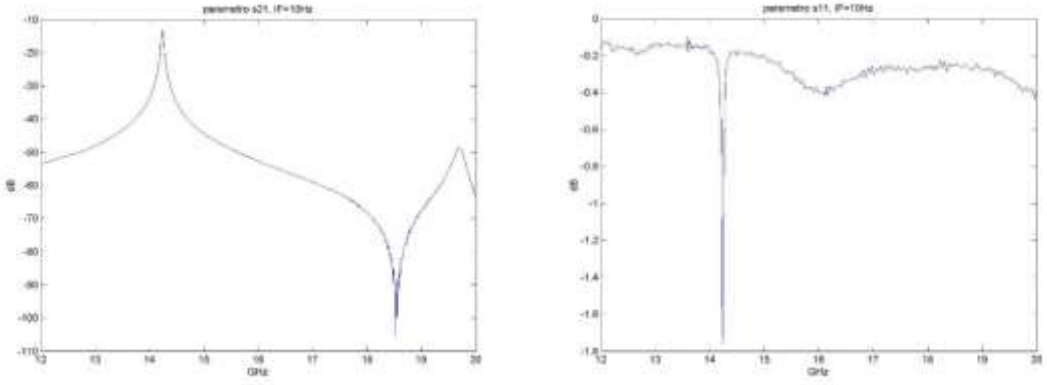

Figure 19. *Measured values of s_{11} and s_{21} between 12 GHz and 20 GHz with IF = 10 Hz.*

In this way the quality factor Q of the first resonant mode (fundamental mode) is estimated as $\omega_{ris}/\Delta\omega_{-3dB}$, where ω_{ris} is the angular frequency under resonant conditions and $\Delta\omega_{-3dB}$ is the difference between the angular frequencies at the right and the left of the resonant frequency at which s_{21} decreases of 3 *dB* with respect to the peak value. Thus the measured *Q*-factor is 352.98. The second resonant peak at 19.7 *GHz*, is smaller and wider than the first, placed at about 5 *GHz* of distance. The quality factor *Q* of this peak is about 109.44 and, consequently, lower than that obtained for the first mode, as expected.

3. CONCLUSION

The success of photonic crystals is related to the possibility to excite modes with very low losses in periodic structures, with strong index contrast, and to achieve a strong light confinement and to reflect all the wavelengths inside the bandgap.

PBG allow to make several high perfomance devices, such as waveguides, filters, optical fibers, resonant cavities, laser with low threshold.

In this paper, after a brief description of operation principle of photonic crystals, we presented a review of the most important photonic crystals devices, describing the main steps required to model and design resonant cavities and particle accelerators.

In particular a PBG-based resonant cavity has been designed, realized and measured. Moreover, this cavity is able to accelerate hadrons, heavy particles, utilized to fight against deep-sided cancer. In fact this technique [18], named *hadrontherapy*, seems to be the main method able to replace radiosurgery, which is not always incisive and sometimes leads up to side effects.

ACKNOWLEDGEMENT

The authors would like to thank the referee for useful and helpful comments and suggestions.

DECLARATIONS

Ethical Approval. The authors declare that there are no animal studies in this work.

Conflict of Interest. The authors declare that they have no conflict of interest.

Author Contributions. First author gave the first idea of investigation, concept and modeling. The methodology has been done by the second author, which also wrote the paper.

Funding. The authors declare that no funds, grants, or other support were received during the preparation of this manuscript.

Data availability. There is no data set used.

REFERENCES

1. P. Yeh, A. Yariv, Chi-S. Hong, Electromagnetic propagation in periodic stratified media. I. General theory, *J. of the Optical Society of America*, 67(4) (1977) 423-438, doi:10.1364/JOSA.67.000423.
2. W. Huang, J. Hong, J., A transfer matrix approach based on local normal modes for coupled waveguides with periodic perturbations, *Journal of Lightwave Technology*, 10(10) (1992) 1367-1375, doi:10.1109/50.166778.
3. J. B. Pendry, Calculating photonic band structure, *Journal of Physics: Condensed Matter*, 8 (1996) 1085-1108, doi**:**10.1088/0953-8984/8/9/003.
4. D. Atkin, P. Sk. Russel, T. Birks, P. J. Roberts, Photonic band structure of guided bloch modes in high index films fully etched through with periodic microstructure, *Journal of Modern Optics*, 43(5) (1996) 1035-1053, doi:10.1080/09500349608233264.

5. R. M., de Ridder, R. Stoffer, Applicability of the finite-difference time-domain method to photonic crystal structures, *AIP Conference Proceedings*, 560 (2001) 99-106, doi:10.1063/1.1372719.
6. J. Ctyroky, S. Helfert, R. Pregla, Analysis of a deep waveguide Bragg grating, *Optical and Quantum Electronics*, 30 (1998) 343-358, doi:10.1023/A:1006964000620.
7. J. Yonekura, M. Ikeda, T. Baba, Analysis of finite 2D photonic crystals of columns and lightwave devices using the scattering matrix method, *Journal of Lightwave Technology*, 17(8) (1999) 1500-1508, doi: 10.1109/50.779177.
8. A. Giorgio, A. G. Perri, M. N. Armenise, Very fast and accurate modeling of multilayer waveguiding photonic bandgap structures, *Journal of Lightwave Technology*, 19(10) (2001) 1598-1613, doi: 10.1109/50.956148.
9. Xin-Y. Lei, H. Li, F. Ding, W. Zhang, Nai-B. Ming, Novel application of a perturbed photonic crystal: High-quality filter, *Applied Physics Letters*, 71(20) (1997) 2889-2891, doi:10.1063/1.120207.
10. E. Yablonovitch, Photonic band-gap structures, *J. of the Optical Society of America B*, 10(2) (1993) 283-295, https://doi.org/10.1364/JOSAB.10.000283.
11. E. Yablonovitch, Photonic Crystals, *Journal of Modern Optics*, 41(2) (1994) 173-194, https://doi.org/10.1080/09500349414550261.
12. R. Diana, A. Giorgio, R. Marani, V. M. N. Passaro, A. G. Perri, A Model to optimize a microwave PBG accelerator based on generic unit cell, *JEOS, Journal of European Optical Society, Rapid Publications*, 2 (2007) 07006, doi: 10.2971/jeos.2007.07006.
13. A. Giorgio, D. Pasqua, A. G. Perri, Multiple defect characterization in finite-size waveguiding photonic bandgap structures, *IEEE Journal of Quantum Electronics*, 39(12) (2003) 1537-1547, doi: 10.1109/JQE.2003.819543.
14. A. Giorgio, D. Pasqua, A. G. Perri, Modelling PBG devices to DWDM filters design, *International Journal of Numerical Modelling*, 17(2) (2004) 85-103, https://doi.org/10.1002/jnm.525.
15. R. Diana, A. Giorgio, A. G. Perri, Theoretical characterization of multilayer photonic crystals having a 2D periodicity, *International Journal of Numerical Modelling*, 18(5) (2005) 365-382, https://doi.org/10.1002/jnm.584.
16. M. A. Shapiro, W. J. Brown, I. Mastovsky, J. R. Sirigiri, R. J. Temkin, 17 GHz photonic band gap cavity with improved input coupling, *Physical Review Accelerators and Beams*, 4 (2001) 1-6, https://doi.org/10.1103/PhysRevSTAB.4.042001.
17. Agilent AN1287-2, Exploring the architectures of Network Analyzers, *Application Notes*, (2004).
18. R. Marani, A.G. Perri, Modelling and Design of Photonic Bandgap Devices: a Microwave Accelerating Cavity for Cancer Hadrontherapy, in *Microwave and Millimeter Wave Technologies: from Photonic Bandgap Devices to Antennas and Applications*, IN-TECH Online, (2010) 431-450, ISBN 978-953-7619-66-4.